Paramagnetic NMR study of Cu^{2+}–IDA complex localization on a protein surface and its application to elucidate long distance information

Makoto Nomura[a], Toshitatsu Kobayashi[a], Toshiyuki Kohno[b], Kenichiro Fujiwara[c], Takeshi Tenno[d], Masahiro Shirakawa[c], Itsuko Ishizaki[a], Kazuo Yamamoto[e], Toshifumi Matsuyama[e], Masaki Mishima[a], Chojiro Kojima[a,*]

[a]*Laboratory of Biophysics, Graduate School of Biological Science, Nara Institute of Science and Technology, 8916-5 Takayama, Ikoma, Nara 630-0192, Japan*
[b]*Mitsubishi Kagaku Institute of Life Sciences (MITILS), Machida, Tokyo 194-8511, Japan*
[c]*Graduate School of Integrated Science, Yokohama City University, Tsurumi, Yokohama 230-0054, Japan*
[d]*Graduate School of Science and Engineering, Ehime University, Matsuyama, Ehime 790-8577, Japan*
[e]*Division of Cytokine Signaling, Department of Molecular Microbiology and Immunology, Nagasaki University Graduate School of Biomedical Sciences, 1-12-4 Sakamoto, Nagasaki 852-8523, Japan*

Received 10 March 2004; revised 12 April 2004; accepted 13 April 2004

Available online 27 April 2004

Edited by Thomas L. James

Abstract The paramagnetic metal chelate complex Cu^{2+}-iminodiacetic acid (Cu^{2+}–IDA) was mixed with ubiquitin, a small globular protein. Quantitative analyses of ^{1}H and ^{15}N chemical shift changes and line broadenings induced by the paramagnetic effects indicated that Cu^{2+}–IDA was localized to a histidine residue (His68) on the ubiquitin surface. The distances between the backbone amide proton and the Cu^{2+} relaxation center were evaluated from the proton transverse relaxation rates enhanced by the paramagnetic effect. These correlated well with the distances calculated from the crystal structure up to 20 Å. Here, we show that a Cu^{2+}–IDA is the first paramagnetic reagent that specifically localizes to a histidine residue on the protein surface and gives the long-range distance information.

Keywords: NMR; Surface histidine; Cu^{2+}–IDA; Paramagnetic relaxation; Pseudo-contact shift; Non-metal protein

1. Introduction

In the field of biological NMR, long-range distance constraints are required for large-size multi-domain proteins and high-throughput structure determinations. Paramagnetic metals have useful properties, such as paramagnetic relaxation enhancement and pseudo-contact shift, both of which affect the NMR signals over long-range distances. For metal proteins and metal–drug–DNA complexes, these paramagnetic effects have been successfully utilized as long-range constraints in structure determinations [1–7].

Kay and co-workers [8,9] developed a method to evaluate the distance between the backbone amide proton and Cu^{2+} using the proton transverse relaxation rate enhanced by the paramagnetic effect for non-metal proteins. The method relies on localizing the paramagnetic ion to a modified target protein such as possessing a specially designed ATCUN motif tag [8,9]. Dvoretsky et al. [10] used the amide proton longitudinal relaxation rates for Mn^{2+} that was localized by mutating an amino acid of the target protein to cysteine followed by covalent modification of this residue using thiol-reactive EDTA. Both methods rely on mutation of the target protein to localize the paramagnetic metal, a procedure that may result in structural changes of the target protein.

Cu^{2+}-iminodiacetic acid (Cu^{2+}–IDA), a metal chelate complex, is an established reagent used in the area of immobilized metal ion affinity chromatography (IMAC) [11]. Immobilized Cu^{2+}–IDA on a solid support specifically binds to histidine residues ($K_d = 10^{-5}$–10^{-4} M) [11–14], and has been used to purify various protein and DNA molecules [11,15]. Other applications involving the use of Cu^{2+}–IDA IMAC have dealt with investigations concerning the structure–function relationship of proteins, which have functional histidine residues [16,17]. Although there are many applications, the precise localization of Cu^{2+}–IDA on the protein surface has not been well characterized [11,12].

Here, the localization of Cu^{2+}–IDA on three different protein surfaces was examined using chemical shift changes, line broadenings and ^{1}H transverse relaxation rate enhancements induced by the paramagnetic effects of Cu^{2+}. The proteins examined were ubiquitin, which has one histidine residue (His68) on the surface, and two other proteins that contain a C-terminal poly histidine tag, the ubiquitin-like domain of human HR23B (HR23B UbL) and the DNA binding domain of human interferon regulatory factor 4 (IRF4 DBD). The potential acquisition of long-range distance constraints was also examined.

2. Materials and methods

2.1. Sample preparation

Recombinant human ubiquitin was expressed in *Escherichia coli* BL21(DE3) as a GST-fusion protein. Following the addition of isopropyl β-D-thiogalactoside, protein expression was induced for 8 h at 30 °C in minimal medium containing ^{15}N-labeled ammonium chloride. Cells were suspended in 50 mM Tris–HCl (pH 8.0), 100 mM KCl and 1 mM Pefabloc SC (Roche). The suspension was lysed by sonication,

* Corresponding author. Fax: +81-743-72-5579.
E-mail address: kojima@bs.aist-nara.ac.jp (C. Kojima).

0014-5793/$22.00
doi:10.1016/j.febslet.2004.04.023

ultra-centrifuged, and the supernatant was loaded onto a glutathione–Sepharose 4B column (Amersham). Elution was performed with 50 mM Tris–HCl (pH 8.0), 100 mM KCl and 30 mM glutathione. The GST–ubiquitin fraction was loaded onto a Superdex 26/60 75 pg (Amersham) gel filtration column equilibrated with 50 mM phosphate (pH 6.5), 50 mM KCl and 1 mM Pefabloc SC. The eluted GST–ubiquitin fraction was then cleaved with PreScission protease (Amersham) and loaded onto a gel filtration column. The final NMR buffer consisted of 50 mM phosphate (pH 6.7) and 200 mM KCl. The expression and purification of HR23B UbL and IRF4 DBD was performed as previously described [18].

2.2. NMR spectroscopy

The stock solution of Cu^{2+}–IDA consisted of 12.5 mM $CuCl_2$, 13.8 mM IDA, 50 mM phosphate and 200 mM KCl (pH 2.2). Following the addition of this stock solution to 0.1 or 1 mM ubiquitin, 0.1 mM HR23B UbL, and 0.5 mM IRF4 DBD, the pH of the sample solution was adjusted to pH 6.7. The ratio of Cu^{2+}–IDA/protein was 0.4 for each unless otherwise noted.

All NMR data were obtained on a Bruker DRX800 spectrometer operating at 800 MHz with a triple-resonance probe head equipped with a XYZ-gradient unit. The ^{1}H–^{15}N HSQC spectra were collected at 293 K, with 2048 (t2) times 150 (t1) complex points and spectral widths of 14 kHz (^{1}H) and 1.6 kHz (^{15}N) with carrier positions at 4.7 and 121.8 ppm, respectively. A $\pi/2$ shifted sine-bell window function was applied before zero-filling and Fourier transformation. The processing was performed using the NMRPipe package [19], while chemical shifts, linewidths and peak volumes were measured using Sparky software [20]. The transverse relaxation rates were obtained using a ^{1}H–^{15}N HSQC based spin echo experiment with a shaped refocusing pulse which was successfully used to obtain long-range distance information with the ATCUN Cu^{2+} system [8]. The relaxation delay times were 8.5, 11, 13.5, 16, 18.5, 21, 23.5, 28.5, 31, 33.5, 38.5, and 48.5 ms for Cu^{2+}–IDA–ubiquitin, and 8.5, 11, 13.5, 16, 18.5, 21, 23.5, 28.5, 33.5, 38.5, 48.5, and 68.5 ms for free ubiquitin.

2.3. Data analyses

Linewidth and chemical shift change. Linewidths were measured for 1 mM ubiquitin samples with and without 0.4 mM Cu^{2+}–IDA. The differences in linewidth were then calculated. When the Cu^{2+}–IDA–ubiquitin peak was not found compared to free ubiquitin ($S/N < 5$), the difference in linewidth was set to the maximum value of 50 Hz. Chemical shift differences of samples with and without Cu^{2+}–IDA were calculated and averaged for three independent experiments. The differences in linewidth and chemical shift values were mapped to the PDB (1UBI).

Paramagnetic ^{1}H relaxation enhancements. Three independent relaxation rate measurements of the 1 mM ubiquitin sample complexed with 0.4 mM Cu^{2+}–IDA were performed. The differences between the transverse relaxation rates with and without Cu^{2+}–IDA were calculated and averaged. The mean values of three experiments were fitted to the relation $R_{2M} = a/r^6 + b$ by non-linear fitting using Mathematica 4.2 (Wolfram) with error bar dependent weights, where R_{2M} is the transverse relaxation rate enhanced by the paramagnetic effects, r is the distance between the target proton and the relaxation center, and a and b are constants. The amide proton position was obtained from the PDB (1UBI) for the residue with the generalized order parameter $S^2 > 0.7$ [21] and the relaxation center position (assumed as Cu^{2+} atom position) was optimized.

3. Results

3.1. Localization and interaction of Cu^{2+}–IDA with ubiquitin

^{1}H–^{15}N HSQC experiments were performed in an effort to evaluate the interaction of Cu^{2+}–IDA with ubiquitin. Titration experiments using Cu^{2+}–IDA with 0.1 and 1 mM ubiquitin solutions resulted in dose-dependent and site-specific line broadenings and shifts. The localization of Cu^{2+}–IDA on the protein was not due to the presence of ionic interactions, but due to some type of coordination to the protein [16,22], since the addition of 200 mM KCl had no effect. The linewidth differences between Cu^{2+}–IDA–ubiquitin and free ubiquitin were mapped to the 3D structure of ubiquitin as shown in Fig. 1 (left), and strongly suggest that Cu^{2+}–IDA bound to ubiquitin around His68. The chemical shift differences up to 30 ppb (25 Hz) were also mapped (Fig. 1, right), supporting the presence of a specific binding site close to His68. At pH 5.0, these line broadenings and shifts were not observed even though the Cu^{2+}–IDA is stable at this pH [16,22]. This result is consistent with the notion that the imidazole nitrogen of histidine ($pK_a = 6.04$) acts as the potential electron donor for Cu^{2+}–IDA [16].

Cu^{2+} has four coordination sites. IDA can coordinate to three of these, while the protein coordinates to the remaining site [23]. Other metals such as Fe^{3+}, Co^{2+}, and Ni^{2+} can have four coordination sites, which could be chelated by IDA. ^{1}H–^{15}N HSQC spectra for these paramagnetic metal–IDA–ubiquitin complexes showed no significant line broadenings and chemical shift differences for ^{1}H, however small chemical shift differences (less than one-tenth of those for Cu^{2+}) were observed for ^{15}N around His68. This result is consistent with the notion that the localization of the paramagnetic metal–IDA complex is around His68.

3.2. Paramagnetic relaxation enhancement analysis

Transverse relaxation rates were measured using spin echo experiments based on ^{1}H–^{15}N HSQC spectra in order to obtain long-range distance information. Distances from Cu^{2+} to each amide proton were calculated using the crystal structure (PDB ID, 1UBI) and transverse relaxation rates, and were designated as the calculated and experimental distances, respectively. Using 49 out of 71 amide proton relaxation rates, the Cu^{2+} position was optimized using the Mathematica software to minimize the difference between those distances. The distances from the optimized Cu^{2+} position to N^{δ} and N^{ε} of the His68 imidazole were 5.6 ± 0.6 and 4.5 ± 1.0 Å, respectively (Fig. 2). The *B*-factors for N^{δ} and N^{ε} were 27 and 28

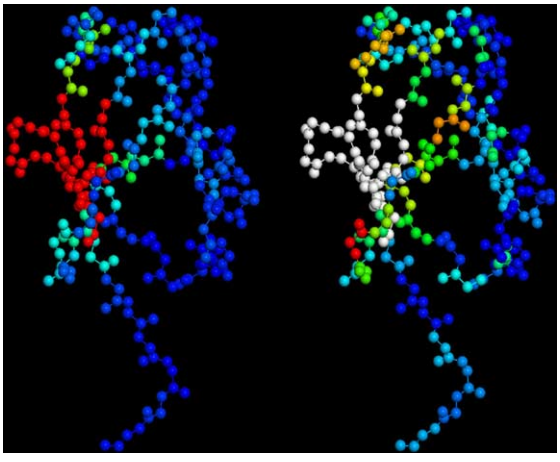

Fig. 1. Line broadenings (left) and peak shifts (right) induced by the Cu^{2+}–IDA complex mapped on the ubiquitin structure. With increasing broadenings and shifts, the color changes from blue to red. Maximum, medium and minimum values (50, 25, and 0 Hz for broadenings, and 30, 15, and 0 ppb for shifts) are colored in red, green and blue, respectively. Intermediate colors such as yellow (between green and red) are given gradually. In the peak shifts (right), white represents disappeared peaks. These pictures were drawn by RASMOL 2.6 [29].

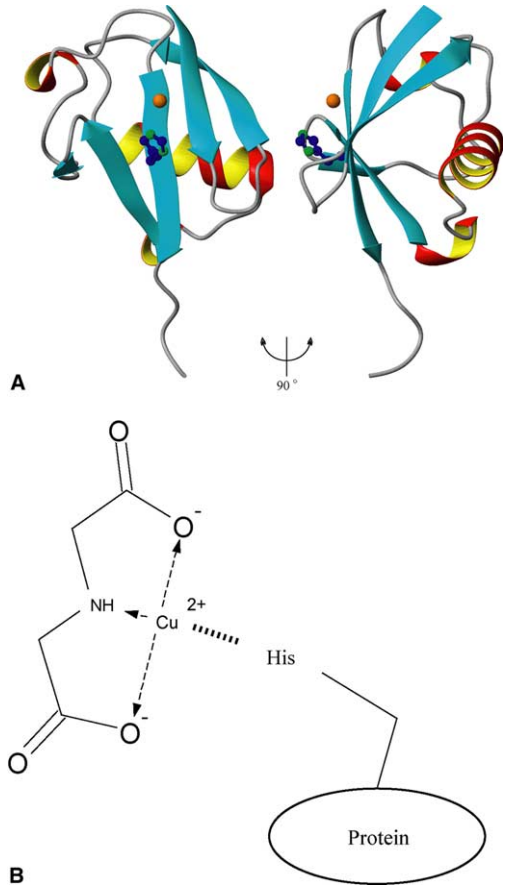

Fig. 2. The ribbon structure of ubiquitin with Cu^{2+} (A), and the chemical structure of IDA and its coordination to Cu^{2+} (B). Side chain of His68 is drawn as a ball-stick model with the two nitrogen atoms colored in green. Cu^{2+} is shown as the gold sphere. The atomic coordinate of Cu^{2+} is optimized, minimizing the calculated and observed proton transverse relaxation rates. The ribbon pictures were prepared by MOLMOL 2k.1 [30].

Å^2, respectively, and much larger than those for the backbone atoms of His68 (2–6 Å^2). This indicates that the imidazole ring is flexible and that those coordinates are less reliable. Additionally, the delocalization of the paramagnetic electron might modulate the relaxation center position [2]. Thus, it is not clear from the distance measurements if His68 does indeed bind the Cu^{2+}–IDA.

The correlation plot between the calculated and experimental distances is shown in Fig. 3. The correlation coefficient R was 0.75. The observed transverse relaxation enhancement was up to 20 Å and the mean error from the calculated values was approximately 3.6 Å. This result highlights the potential in acquiring long-range distance information using the Cu^{2+}–IDA complex, although the precision was not very high.

Relaxation experiments were repeated on samples containing a change in Cu^{2+}–IDA concentration from 0.4 to 0.2 or 0.8 mM. The relaxation data determined were fitted to the theoretical equation and were well converged. The converged coordinates of Cu^{2+} were quite similar to each other for the three data sets (RMSD = 1.3 Å). The experimental distances were correlated with the calculated ones, where $R = 0.67$ and 0.80 for the 0.2 and 0.8 mM samples, respectively.

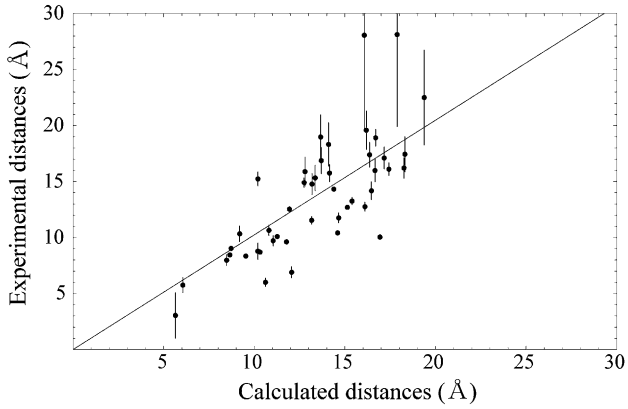

Fig. 3. Correlation plot between calculated and experimental distances from Cu^{2+} to each backbone amide proton of ubiquitin. Calculated distances were taken from the crystal structure. The experimental distances were obtained from the paramagnetic enhancement of the proton transverse relaxation rates.

4. Discussion

The binding between ubiquitin and Cu^{2+}–IDA was evaluated further by EPR. EPR spectra were recorded by a JEOL JES-TE300 X-band spectrometer at 77 K using 2.5 mM Cu^{2+}–IDA. The spectra significantly changed in the presence and absence of ubiquitin ($g_{\|} = 2.27$ and 2.32, $A_{\|} = 15.8$ and 15.9, and $g_{\perp} = 2.06$ and 2.07, respectively). In the ubiquitin titration series, Cu^{2+}–IDA spectra were explained by the weighted sum of only two spectra, i.e., free and 1:1 complex. EPR splitting patterns of Cu^{2+}–IDA complexed with a histidine were quite similar to ubiquitin complex. These data strongly suggest that Cu^{2+}–IDA coordinates to ubiquitin at one specific site, His68.

The localization of Cu^{2+}–IDA on two other proteins was investigated to reveal whether Cu^{2+}–IDA specifically binds to the surface histidine residue. The ^1H–^{15}N HSQC spectra of HR23B UbL and IRF4 DBD with and without Cu^{2+}–IDA clearly demonstrated the site-specific line broadenings and shifts around the histidine residues. Broadening ratios for all proteins examined here are given in Fig. 4. Distance information was not elucidated for HR23B UbL and IRF4 DBD, since the coordinates were not available for the free proteins. A cysteine residue is the potential binding site of Cu^{2+}–IDA, but not examined in this study because of two difficulties. First, Cu^{2+}–IDA complex cannot be used with dithiothreitol (DTT) since a Cu^{1+}-DTT complex is formed [24]. Second, a free cysteine residue decreases protein stability, and the mixture of the Cu^{2+}–IDA and a cysteine forms aggregates. Thus, *N*-ethylmaleimide was used to chemically modify the surface cysteine residue of IRF4 DBD in our experiments. Other paramagnetic metal chelate complexes, such as Mn^{2+}–NTA and Gd^{3+}–EDTA, did not bind specifically to the histidine residues for three proteins possessing a poly hisitidine tag; HR23B UbL, IRF4 DBD and the S5a UbL binding region [18]. These results are consistent with hard-soft-acid-base (HSAB) theory [25–27].

Characteristic properties of the Cu^{2+}–IDA complex, that includes highly specific localization to the histidine residue and the capability of obtaining distance information, offer clear advantages in the analysis of macromolecular intermolecular interactions such as protein–protein, protein–DNA and

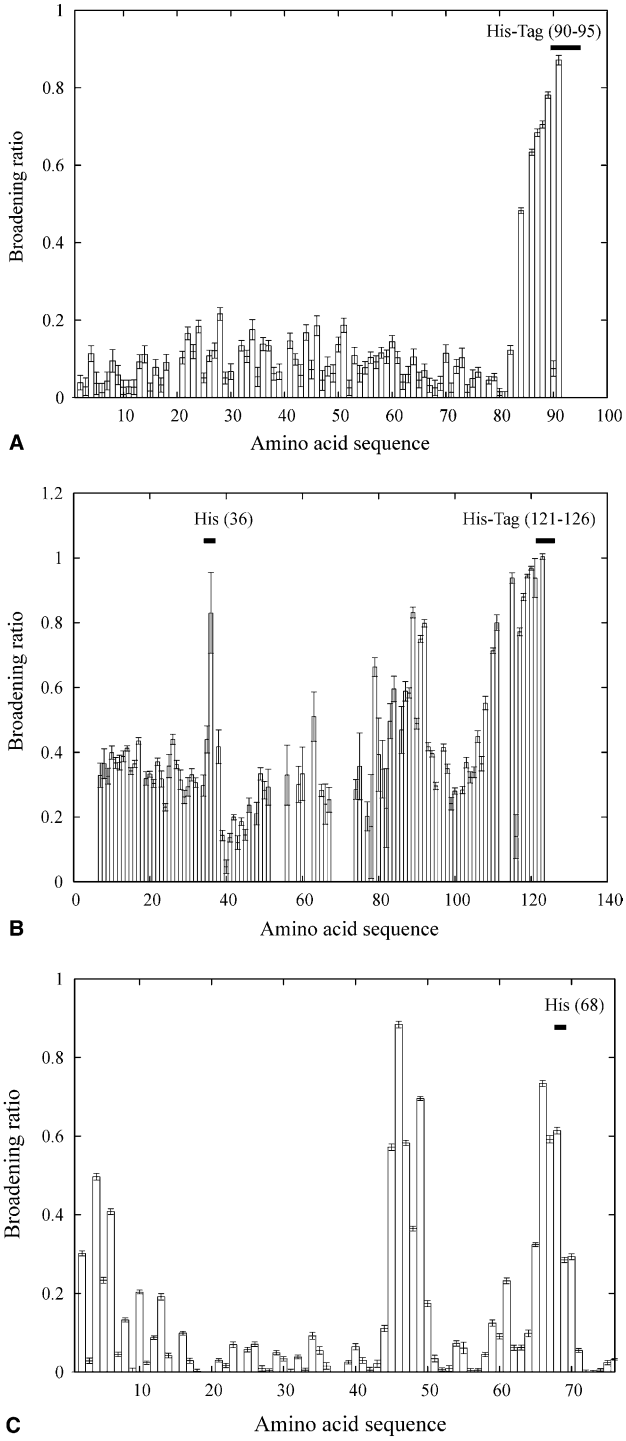

Fig. 4. The broadening ratios of HR23B UbL (A), IRF4 DBD (B), and ubiquitin (C) were plotted against the amino acid sequence. The broadening ratio is defined as $\sqrt{(I-I_0)^2}/\sqrt{I_0^2}$, where I and I_0 represent the peak height with and without Cu^{2+}–IDA (1 equiv.), respectively. The 79th to 92th residues of IRF4 DBD were spatially close to His36 in the modeled structure.

protein–ligand interactions. Hansen et al. [28] employed the paramagnetic longitudinal proton relaxation enhancement of a metal protein to detect transient intermolecular protein–protein interactions. Mal et al. [9] utilized the ATCUN Cu^{2+} system to detect protein–protein interactions. Therefore, transient interactions showing few intermolecular NOEs can be the subject of investigation using Cu^{2+}–IDA provided that a surface histidine residue is located near the interface.

Another potential application of the Cu^{2+}–IDA complex can be in the investigation of membrane proteins. Membrane proteins are usually solubilized within a detergent micelle and it is difficult to construct an expression system. Distance information in general is insufficient,and any specific modification appears daunting,to say the least. We applied the Cu^{2+}–IDA system to a membrane protein solubilized within a detergent,and the ^{1}H–^{15}N HSQC spectrum showed site-specific line broadenings and shifts (Okuda et al., unpublished results). These results indicate the potential application of the Cu^{2+}–IDA system in the study of membrane protein structures.

In conclusion, all examined paramagnetic metal chelate complexes were not localized to a specific site on the protein surface with exception of Cu^{2+}–IDA,that was specifically localized to His68 on the ubiquitin surface. This feature of Cu^{2+}–IDA was successfully utilized to elucidate long-range distance information from proton transverse relaxation enhancements. Cu^{2+}–IDA could also be used in conjunction with poly histidine tagged proteins,but it may be difficult to obtain precise distance constraints for proteins possessing many histidine residues. Application of the Cu^{2+}–IDA method to the investigation of surface histidine residues is a technique worthy of consideration, since surface histidine residues are frequently found in many proteins and can play important roles in many biochemical reactions and interactions.

Acknowledgements: We thank H. Okuda for his assistance, Prof. J.L. Markley and Prof. C. Griesinger for their critical comments, and Prof. S. Suzuki for his helpful comments on EPR analyses. This work was supported in part by Grants-in-Aid for 21st Century COE Research and Scientific Research, a Grant for the National Project on Protein Structural and Functional Analyses from MEXT (the Japanese Ministry of Education, Culture, Sports, Science and Technology), a Kaneko Narita Research Grant of Protein Research Foundation and a Grant from the Yamada Science Foundation.

References

[1] Bertini, I., Donaire, A., Jimenez, B., Luchinat, C., Parigi, G., Piccioli, M. and Poggi, L. (2001) J. Biomol. NMR 21, 85–98.
[2] Bertini, I., Luchinat, C. and Parigi, G. (2001) Solution NMR of Paramagnetic Molecules. Elsevier, Amsterdam.
[3] Bertini, I., Luchinat, C. and Piccioli, M. (2001) Methods Enzymol. 339, 314–340.
[4] Gochin, M. (1997) J. Am. Chem. Soc. 119, 3377–3378.
[5] Gochin, M. (1998) J. Biomol. NMR 12, 243–257.
[6] Kikuchi, J., Iwahara, J., Kigawa, T., Murakami, Y., Okazaki, T. and Yokoyama, S. (2002) J. Biomol. NMR 22, 333–347.
[7] Arnesano, F., Banci, L., Bertini, I., Felli, I.C., Luchinat, C. and Thompsett, A.R. (2003) J. Am. Chem. Soc. 125, 7200–7208.
[8] Donaldson, L.W., Skrynnikov, N.R., Choy, W.Y., Muhandiram, D.R., Sarkar, B., Forman-Kay, J.D. and Kay, L.E. (2001) J. Am. Chem. Soc. 123, 9843–9847.
[9] Mal, T.K., Ikura, M. and Kay, L.E. (2002) J. Am. Chem. Soc. 124, 14002–14003.
[10] Dvoretsky, A., Gaponenko, V. and Rosevear, P.R. (2002) FEBS Lett. 528, 189–192.
[11] Gaberc-Porekar, V. and Menart, V. (2001) J. Biochem. Biophys. Methods 49, 335–360.
[12] Yip, T.T., Nakagawa, Y. and Porath, J. (1989) Anal. Biochem. 183, 159–171.
[13] Hutchens, T.W. and Yip, T.T. (1990) Anal. Biochem. 191, 160–168.
[14] Mrabet, N.T. (1992) Biochemistry 31, 2690–2702.

[15] Murphy, J.C., Jewell, D.L., White, K.I., Fox, G.E. and Willson, R.C. (2003) Biotechnol. Progr. 19, 982–986.
[16] Berna, P.P., Mrabet, N.T., Van Beeumen, J., Devreese, B., Porath, J. and Vijayalakshmi, M.A. (1997) Biochemistry 36, 6896–6905.
[17] Jiang, K.Y., Pitiot, O., Anissimova, M., Adenier, H. and Vijayalakshmi, M.A. (1999) Biochim. Biophys. Acta 1433, 198–209.
[18] Fujiwara, K., Tenno, T., Sugasawa, K., Jee, J.G., Ohki, I., Kojima, C., Tochio, H., Hiroaki, H., Hanaoka, F. and Shirakawa, M. (2004) J. Biol. Chem. 279, 4760–4767.
[19] Delaglio, F., Grzesiek, S., Vuister, G.W., Zhu, G., Pfeifer, J. and Bax, A. (1995) J. Biomol. NMR 6, 277–293.
[20] Goddard, T.D. and Kneller, D.G. (1999) Sparky 3. University of California, San Francisco.
[21] Schneider, D.M., Dellwo, M.J. and Wand, A.J. (1992) Biochemistry 31, 3645–3652.
[22] Sulkowski, E. (1987) in: Protein Purification: Micro to Macro (Burgess, R.R., Ed.), pp. 149–162, Alan R. Liss Inc, New York.
[23] Hochuli, E., Dobeli, H. and Schacher, A. (1987) J. Chromatogr. 411, 177–184.
[24] Kr zel, A., Lesniak, W., Jezowska-Bojczuk, M., Mlynarz, P., Brasun, J., Kozlowski, H. and Bal, W. (2001) J. Inorg. Biochem. 84, 77–88.
[25] Aime, S., D'Amelio, N., Fragai, M., Lee, Y.M., Luchinat, C., Terreno, E. and Valensin, G. (2002) J. Biol. Inorg. Chem. 7, 617–622.
[26] Kemple, M.D., Ray, B.D., Lipkowitz, K.B., Prendergast, F.G. and Nageswara Rao, B.D. (1988) J. Am. Chem. Soc. 110, 8275–8787.
[27] Petros, A.M., Mueller, L. and Kopple, K.D. (1990) Biochemistry 29, 10041–10048.
[28] Hansen, D.F., Hass, M.A., Christensen, H.M., Ulstrup, J. and Led, J.J. (2003) J. Am. Chem. Soc. 125, 6858–6859.
[29] Sayle, R.A. and Milner-White, E.J. (1995) Trends Biochem. Sci. 20, 374.
[30] Koradi, R., Billeter, M. and Wuthrich, K. (1996) J. Mol. Graph. 14, 51–55, 29–32.